

PETROGENESIS OF THE Pd-RICH INTRUSION AT SALT CHUCK, PRINCE OF WALES ISLAND: AN EARLY PALEOZOIC ALASKAN-TYPE ULTRAMAFIC BODY

ROBERT A. LONEY

U.S. Geological Survey, 345 Middlefield Road, Menlo Park, California 94025, U.S.A.

GLEN R. HIMMELBERG

U.S. Geological Survey and Department of Geology, University of Missouri, Columbia, Missouri 65211, U.S.A.

ABSTRACT

The early Paleozoic Salt Chuck intrusion has petrographic and chemical characteristics that are similar to those of Cretaceous Alaskan-type ultramafic-mafic bodies. The Salt Chuck intrusion is markedly discordant to the structure of the early Paleozoic Descon Formation, in which it has produced a rather indistinct contact aureole a few meters wide. Field relationships and sequences of cumulus minerals indicate that the two rock types, magnetite clinopyroxenite and gabbro, are related by fractional crystallization. All analyzed samples are feldspathoid-normative, a result of the high proportion of the esseneite component of clinopyroxene and not an indication of crystallization from a silica-undersaturated magma. The Mg# of the modal clinopyroxene ranges from 0.937 to 0.831, consistent with a normal trend of fractional crystallization. Mineral assemblages, sequence of crystallization, and mineral chemistry suggest that the intrusion crystallized under low pressures (≈ 2 kbar) with oxidation conditions near those of the NNO buffer, from a hydrous, silica-saturated, orthopyroxene-normative parental magma. The dominance of Pd over Pt [average $Pt/(Pt+Pd) = 0.06$] in the Salt Chuck intrusion contrasts sharply with the general dominance of Pt over Pd [average $Pt/(Pt+Pd) = 0.59$] in other Alaskan-type bodies. There are also generally higher levels of PGE and sulfide concentrations in the Salt Chuck deposit. Sulfides in the Salt Chuck intrusion are substantially more Cu- and Pd-rich than magmatic sulfides in other ultramafic rocks. The Salt Chuck deposit was probably formed by a two-stage process: (1) a stage of magmatic crystallization in which the sulfides and PGE accumulated in a disseminated manner in cumulus deposits, possibly largely in the gabbro, and (2) a later magmatic-hydrothermal stage during which the sulfides and PGE were remobilized and concentrated in veins and fracture-fillings, largely in the magnetite clinopyroxenite but controlled by the complex magnetite clinopyroxenite - gabbro contact. In this model, the source of the sulfides and PGE was the magma that produced the Salt Chuck intrusion.

Keywords: Alaskan-type intrusion, ultramafic rocks, platinum-group elements, sulfides, arc magmatism, early Paleozoic, Salt Chuck, Alaska.

SOMMAIRE

Le complexe intrusif de Salt Chuck, sur l'île du Prince de Galles, en Alaska, d'âge paléozoïque précoce, possède des caractéristiques pétrographiques et géochimiques semblables à celles des massifs ultramafiques à mafiques de type Alaska, d'âge crétacé. Le complexe de Salt Chuck montre une grande discordance structurale avec les roches de la Formation Descon, sur lesquelles il a imposé une auréole de contact plutôt indistincte. Les relations de terrain et les séquences de cumulats indiquent que les roches mafiques et ultramafiques sont liées par processus de cristallisation fractionnée. Tous les échantillons analysés possèdent de la néphéline normative, résultat de la teneur élevée du pôle esseneite dans le clinopyroxène, et non une indication d'un magma sous-saturé en silice. La valeur de Mg# du clinopyroxène modal s'étale entre 0.937 et 0.831, et définit un tracé normal de fractionnement igné. Les assemblages de minéraux, la séquence de cristallisation, et la composition des minéraux font penser que le complexe intrusif a cristallisé à pression relativement faible (≈ 2 kbar), à une fugacité d'oxygène proche de celle du tampon NNO, à partir d'un magma parental hydraté, saturé en silice, et donc à orthopyroxène normatif. La prédominance du Pd au Pt [$Pt/(Pt+Pd)$ moyen: 0.06] dans ces roches contraste fortement avec la dominance du Pt par rapport au Pd dans les autres massifs de type Alaska [$Pt/(Pt+Pd)$ moyen: 0.59]. De plus, les roches de Salt Chuck contiennent des niveaux plus élevés des éléments du groupe du platine (EGP) et des sulfures. Les sulfures ici sont plus riches en Cu et en Pd que les sulfures magmatiques des autres roches ultramafiques. Nous proposons un modèle de formation du gisement en deux étapes: 1) stade magmatique précoce, au cours duquel les sulfures et les EGP ont été déposés de façon disséminée dans les cumulats, et 2) stade hydromagmatique, au cours duquel la minéralisation a été concentrée dans la clinopyroxénite à magnétite près de son contact avec le gabbro. Dans ce modèle, les sulfures et les EGP seraient issus du magma parental.

(Traduit par la Rédaction)

Mots-clés: intrusion de type Alaska, roches ultramafiques, éléments du groupe du platine, sulfures, magmatisme d'arc, Paléozoïque précoce, Salt Chuck, Alaska.

INTRODUCTION

The Pd-bearing intrusion at Salt Chuck on Prince of Wales Island is spatially part of the belt of ultramafic–mafic bodies that extends from Klukwan to Duke Island in southeastern Alaska (Fig. 1). These bodies have been known for many years because of economic interest in chromium, iron, nickel, copper, and platinum-group elements (PGE) (Buddington & Chapin 1929, Kennedy & Walton 1946, Walton 1951). In 1960 these bodies were recognized as a special class of intrusions, referred to as Alaskan-type ultramafic bodies (Noble & Taylor 1960, Taylor & Noble 1960). The distribution and age of the bodies were further refined by Lanphere & Eberlein (1966), Taylor (1967), Lanphere (1968), Brew & Morrell (1984), and Himmelberg *et al.* (1986). Lanphere & Eberlein (1966) reported K/Ar ages for these bodies, based on biotite and hornblende, that range from 100 to 110 Ma. Although the generalized maps of some of these investigators included the Salt Chuck intrusion and smaller ultramafic–mafic bodies on nearby islands, none of these bodies was included in the original descriptions and sampling for age determinations. Recently, Loney *et al.* (1987) reported a much older K–Ar age for biotite (about 429 Ma) in the Salt Chuck body. Similar K–Ar ages were obtained on biotite and hornblende by M.A. Lanphere (written communication, 1989) for ultramafic bodies on Dall Island (400 Ma) and Sukkwan Island (440 Ma) (Fig. 1). These bodies represent early Paleozoic magmatic arc activity similar to the late Cretaceous activity that produced the better known ultramafic bodies originally defined as Alaskan-type intrusions (Lanphere & Eberlein 1966, Taylor 1967). The DNAG Time Scale (Palmer 1983) is used in this paper to relate radiometric ages with the geological time-scale.

Other episodes of Alaskan-type, magmatic arc emplacement have been reported from western North America. Gray *et al.* (1986) described three suites of postorogenic, ultramafic to gabbroic rocks in the Klamath Mountains of California and Oregon that were intruded in the Late Jurassic (142–163 Ma). Findlay (1969) described the Tulameen ultramafic–gabbroic complex in British Columbia as an Alaskan-type body, which, according to K–Ar ages (175–186 Ma), was intruded in the Jurassic (Leech *et al.* 1963, Roddick & Farrar 1971, 1972). Recent U–Pb zircon ages (204–212 Ma) suggest that it may be as old as Triassic (Ruble & Parrish 1990). These occurrences indicate that the petrological and tectonic environment that produced the Alaskan-type intrusions was not unique.

Unlike the late Cretaceous Alaskan-type ultramafic bodies, the Salt Chuck intrusion is the host for an economic Cu–Au–Pd ore deposit (Gault 1945, Holt *et al.* 1948, Loney *et al.* 1987). The deposit is considered by us to be a magmatic deposit that was remobilized and concentrated by later magmatic and hydrothermal processes during a single intrusive event. Hence, the petro-

genesis of the Salt Chuck intrusion bears on the origin of the ore deposit and that of similar ores elsewhere.

It must be emphasized that our work was entirely confined to the surface outcrops and, except for the mine dump, our information about the underground is mostly derived from the mine mapping of Gault (1945) and Gault & Wahrhaftig (1992) and chemical data from Silver Glance Resources Inc. Other than at the mine, exposures in the heavily forested area are extremely limited.

REGIONAL SETTING

As can be seen in Figure 1, the Salt Chuck intrusion lies near the western margin of the Klukwan–Duke belt of 100- to 110-Ma Alaskan-type ultramafic bodies (Lanphere & Eberlein 1966, Brew & Morrell 1984), which extends in Alaska from Duke Island on the south to Klukwan on the north, and probably at least 150 km father north to Pyroxenite Creek in the Yukon Territory (Sturrock *et al.* 1980). Among others, the belt includes the ultramafic bodies at Alava Bay, Union Bay, Blashke Islands, Kane Peak, and Haines. This belt cross-cuts the terrane pattern that developed in Late Cretaceous time, and is clearly later (Brew & Morrell 1984, Himmelberg *et al.* 1986). The Salt Chuck body discordantly intrudes the Alexander terrane (early Paleozoic Descon Formation), as do the other roughly coeval ultramafic bodies, and their petrogenesis is related to the early Paleozoic tectonic environment in which they were formed. According to Gehrels & Saleeby (1987a), the Ordovician to Early Silurian plutonic, volcanic, and sedimentary rocks of the Alexander terrane on Prince of Wales Island and nearby islands resemble the lithological assemblage, geochemical characteristics, and regional relations of modern convergent-margin assemblages, indicating that they were formed in a volcanic-arc environment.

The age range of the Salt Chuck and other Paleozoic Alaskan-type bodies (400–440 Ma) overlaps the boundary between the Middle Ordovician to Early Silurian (438–472 Ma) interval of calc–alkaline plutonism and the younger plutonism that is represented by the younger Silurian (418 Ma) sodic leucodiorite of Kassa Inlet, as established by Gehrels & Saleeby (1987b) for southern Prince of Wales Island. Chemically, the ultramafic–mafic bodies of the Salt Chuck type are more compatible with the examples of volcanic-arc, calc–alkaline plutonism than with the sodic plutonic suites. The Salt Chuck intrusion could well be related to the heterogeneous Early Ordovician to Early Devonian ensimatic igneous complex described by Saleeby & Eberlein (1981), which crops out nearby (Fig. 2).

FIELD AND PETROGRAPHIC CHARACTERISTICS OF THE INTRUSION

The Salt Chuck intrusion forms a tadpole-shaped outcrop that trends west–northwest for a distance of 7.3

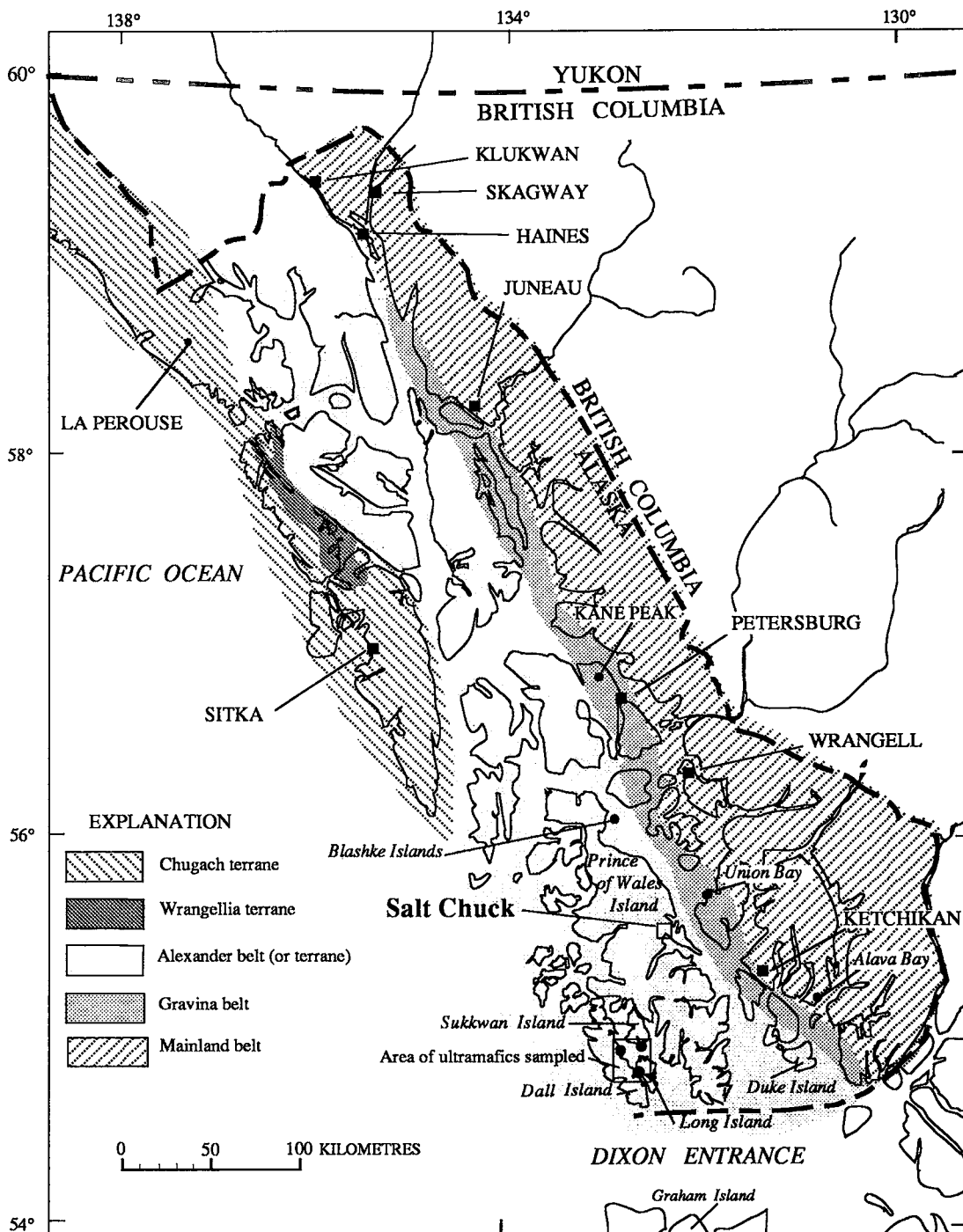
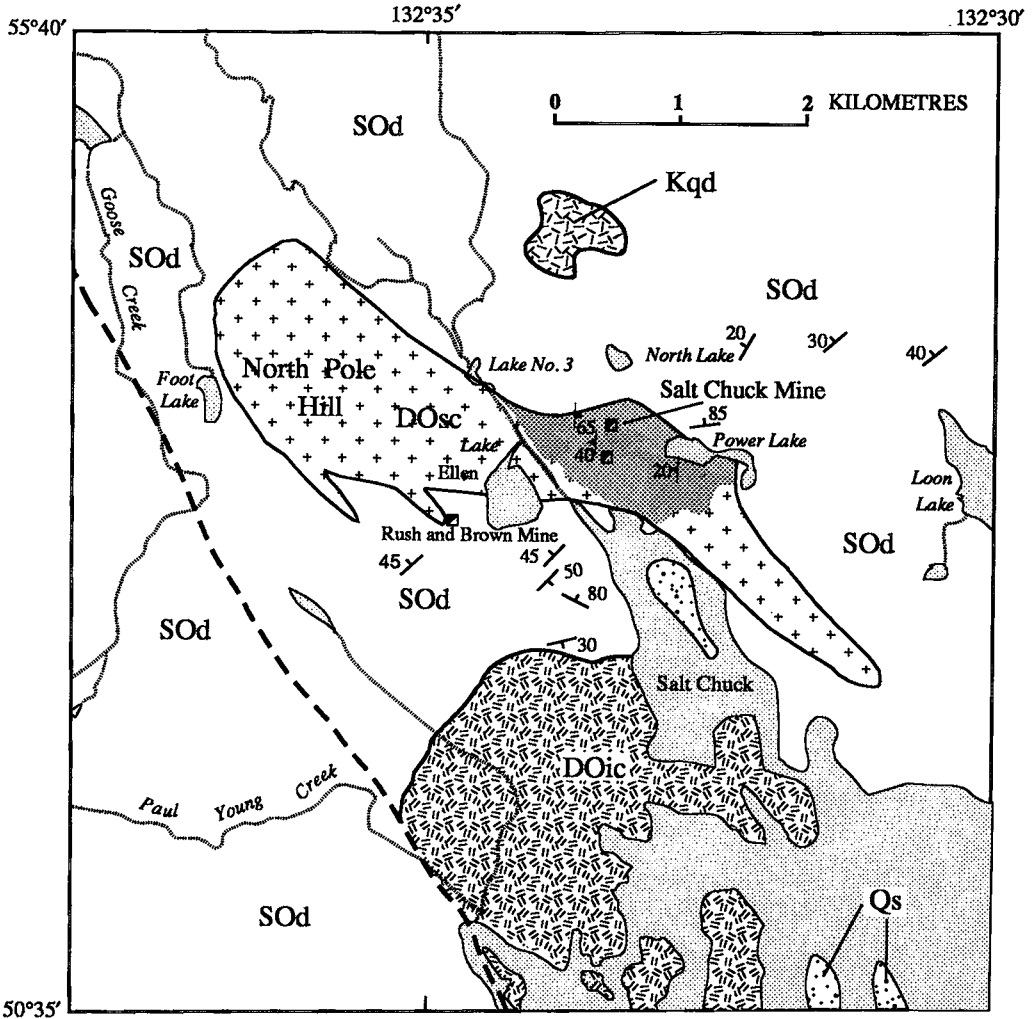




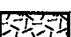

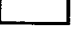






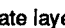

FIG. 1. Map of southeastern Alaska, showing locations of the Salt Chuck intrusion and roughly coeval (early Paleozoic) intrusions sampled by the authors, the Duke-Klukwan ultramafic belt, and major tectonostratigraphic units. Map compiled from Berg *et al.* (1978), Brew & Ford (1984), Himmelberg *et al.* (1986), and Gehrels & Saleeby (1987a).

km; its maximum width is about 1.6 km at its western end (Fig. 2). The location of contacts shown in Figure 2 is virtually the same as mapped by Sainsbury (1961),

who was the first to map the gabbro at North Pole Hill as part of the body. The country rocks consist of basalt flows, pyroclastic rocks, graywacke, and argillite of the



EXPLANATION

-  Lakes, tide-water, and tidal zones
-  Qs Surficial deposits (Quaternary)--Mainly alluvium, tidal mudflat, and glaciofluvial deposits
-  Kqd Quartz diorite porphyry (Cretaceous?)--Contains large plagioclase phenocrysts (Sainsbury 1961)
-  SOd Descon Formation (Lower Silurian and Ordovician)--Mainly graywacke and mudstone with interbedded pillow basalt flows and pyroclastic rocks (Eberlein & Churkin 1970; Eberlein et al. 1983)
-  DOic Ensimatic igneous complex (Early Devonian to Early Ordovician)--Metagneous complex consisting of masses of dioritic-mafic migmatite, and irregular intrusive bodies of hornblende and (or) quartz chloritic magmatite, leucogabbro, trondhjemite, and minor pyroxenite cut by mafic and felsic dike swarms (Saleeby & Eberlein 1981)
-  DOsc Salt Chuck intrusion (Early Devonian? to Early Ordovician)--Sulfide-bearing clinopyroxenite and gabbro with gradational contacts, gb - gabbro, cpx - clinopyroxenite, gbcp - undivided
-  Stream
-  Contact, approximately located
-  Fault, approximately located
-  Shoreline
-  40° Strike and dip of cumulate layering
-  45° Strike and dip of bedding
-  Mine shaft

Descon Formation (Eberlein *et al.* 1983). The actual contact is not exposed, but samples from two outcrops of clinopyroxene–phyric volcanic rocks, approximately 10 meters from the nearest outcrops of the intrusion, show recrystallization of matrix to a granoblastic polygonal association of clinopyroxene, plagioclase, and minor biotite. Other outcrops of country rock further from the intrusion, however, show no evidence of thermal effects by the intrusion.

In general, the bedding in the graywacke and argillite of the Descon Formation strikes northeast and dips moderately to steeply to the northwest, with some reversals, suggesting folding (Fig. 2). The intrusion, therefore, is markedly cross-cutting to the structure in the country rocks, although the poor exposures make it difficult to obtain details.

The Salt Chuck intrusion consists almost entirely of magnetite clinopyroxenite and gabbro (Fig. 2). Our surface observations indicate that the two rock types grade irregularly into one another by a gradual increase in postcumulus plagioclase in the magnetite clinopyroxenite prior to appearance of cumulus plagioclase in gabbro, which is consistent with fractional crystallization of a single magma-batch. Within the mine, however, magnetite clinopyroxenite overlies gabbro (Gault 1945, Gault & Wahrhaftig 1992, Watkinson & Melling 1989), which led Watkinson & Melling (1989) to propose that the magnetite clinopyroxenite intruded the gabbro. The relationships certainly suggest that there may be more than one magnetite clinopyroxenite – gabbro unit. However, rather than igneous intrusion as proposed by Watkinson & Melling (1989), we suggest that the magnetite clinopyroxenite overlying the gabbro may represent the base of a new cyclic unit attributed to emplacement of a new pulse of more primitive magma into the magma chamber.

Mine mapping by Gault (1945) and Gault & Wahrhaftig (1992) shows that the contact between the gabbro and overlying magnetite clinopyroxenite is an irregular synform with subvertical limbs that plunge steeply (45° to 60°) to the southeast. The distance between this contact on opposite limbs is about 100 m. Near this contact, the magnetite clinopyroxenite and gabbro are intertongued (or interlayered) on a scale of about 0.5 to 1.5 m in thickness. On the surface near the mine, we observed lenticular cumulate layers of this scale in magnetite clinopyroxenite and gabbro (Fig. 2), but observations were too few to enable us to relate their orientation to that of the larger-scale structure described in the mine. Gault & Wahrhaftig (1992) constructed a vertical section through the mine, normal to the trend of the synform, about 170 m southeast of the main glory hole. The section shows a distribution of thick magnetite

clinopyroxenite and gabbro units suggestive of alternating antiforms and synforms having axial planes dipping steeply to the southwest, and comparable in scale and orientation to the synform described above.

Most exposures of magnetite clinopyroxenite and gabbro are massive and homogeneous, although isomodal layers 2 to 8 cm thick, distinguished by different proportions of clinopyroxene and plagioclase, are locally present in gabbro. The magnetite clinopyroxenites are clinopyroxene–magnetite cumulates with postcumulus biotite and plagioclase. Most gabbros are anhedral granular or subhedral granular clinopyroxene – plagioclase – magnetite cumulates with postcumulus biotite. Grain size of all the rocks is generally 1–2 mm, with the exception of biotite oikocrysts in magnetite clinopyroxenite, which may be as much as 2 to 3 cm across. Although the rocks are extensively altered and veined by epidote, reasonable estimates of original modal mineralogy are as follows: clinopyroxene, 90% in magnetite clinopyroxenite to 35% in gabbro; plagioclase, less than 1% to 10% in magnetite clinopyroxenite, and 20 to 65% in gabbro; magnetite, generally 5 to 10% in magnetite clinopyroxenite and gabbro, although some gabbros contain as little as 2% magnetite; biotite, 1 to 10% in magnetite clinopyroxenite and gabbro. Only trace amounts of brown to green hornblende are present in some magnetite clinopyroxenites and gabbros, which is markedly different from the case of other Alaskan-type ultramafic rocks, where hornblende is a major and characteristic constituent. Apatite is a ubiquitous accessory mineral in gabbro and present in some magnetite clinopyroxenites. Interstitial K-feldspar was noted in one sample of gabbro. The occurrence of sulfides in the magnetite clinopyroxenite and gabbro is discussed below.

The clinopyroxene is neutral to pale green in color; some grains show concentric optical zoning. Magnetite clinopyroxenite and gabbro show extensive deuteric alteration. Plagioclase in most samples is entirely altered to a mixture of white mica, zoisite or clinozoisite, epidote and, in some cases, minor calcite and prehnite. Biotite is commonly altered to chlorite, epidote, and prehnite. Clinopyroxene remains unaltered except for minor chloritic alteration along cleavage and fractures in some samples.

The magnetite clinopyroxenite exposed at the glory hole in the Salt Chuck mine is intruded by a gabbro dike with diabasic to subophitic texture. An exposure of clinopyroxene – hornblende – biotite diorite with a subhedral granular texture occurs near the contact of the intrusion north of the Salt Chuck mine. The possible genetic relationship of the diabase and diorite to the

magnetite clinopyroxenite and gabbro of the Salt Chuck intrusion is discussed below.

COMPOSITION OF ROCKS AND MINERALS

The chemical composition and CIPW norm for rocks of the Salt Chuck intrusion are given in Table 1. The analyses were obtained by using X-ray fluorescence spectroscopy. FeO and Fe₂O₃ were determined by independent measurement of Fe²⁺ using gravimetric and wet-chemical methods. A petrogenetically significant feature of the intrusion is that all the samples analyzed are feldspathoid-normative; four samples of magnetite clinopyroxenite and two of gabbro are even larnite-normative. The presence of silica-undersaturated components in the norm is a result of the high proportion of the esseneite component (CaFe³⁺AlSiO₆) of clinopyroxene in these rocks (see below). Because the rocks of the Salt Chuck intrusion are cumulates with variable percentages of magnetite, the relationship of whole-rock chemistry to chemical trends due to fractionation is best indicated by the Mg# [$Mg/(Mg+Fe^{2+})$] of the normative silicates.

The Mg# shows a substantial range, from 0.99 to 0.94 in magnetite clinopyroxenite and from 0.92 to 0.82 in gabbro, which is consistent with a normal trend of fractional crystallization. The lower Mg# (0.80) in magnetite clinopyroxenite sample 86GH8A and gabbro sample 86GH7A is attributed to the presence of bornite and chalcopyrite, which also accounts for the slightly low oxide totals. The diabase dike (sample 86GH8B) that intrudes the magnetite clinopyroxenite and the clinopyroxene – hornblende – biotite diorite (sample 86GH14A) are hypersthene-normative and have a normative silicate Mg# of 0.78 and 0.57, respectively. The possible genetic relationship of these two rocks to the Salt Chuck cumulates is discussed below.

Chemical compositions and structural formulas of clinopyroxene, hornblende, and biotite are given in Tables 2 through 4. All minerals were analyzed using the JEOL model 733 Superprobe at Washington University, St. Louis, Missouri. Natural minerals and oxides were used as standards. Matrix corrections were made by the method of Bence & Albee (1968) using the correction factors of Albee & Ray (1970). Because of

TABLE 1. CHEMICAL COMPOSITION AND CIPW NORM OF SAMPLES OF THE SALT CHUCK INTRUSION

Sample	86GH 23A	86GH 25A	86GH 20A	86GH 9B	86GH 8A	86GH 11A	86GH 7A	86GH 1A	86GH 27A	86GH 3B	86GH 8B	86GH 14A
SiO ₂	40.40	41.30	41.40	40.40	36.00	41.10	40.70	40.50	43.30	47.20	46.80	51.40
TiO ₂	0.92	0.90	0.83	0.92	1.31	1.02	0.94	0.74	0.84	0.61	0.71	0.54
Al ₂ O ₃	5.67	5.54	4.72	15.40	12.70	7.35	16.10	18.50	17.00	19.70	14.80	19.00
Fe ₂ O ₃	13.89	12.89	12.56	8.58	10.16	11.33	6.70	7.54	6.79	4.26	3.20	1.48
FeO	8.00	6.57	7.49	5.68	9.11	7.16	6.65	4.91	5.40	3.62	6.93	6.48
MnO	0.21	0.18	0.20	0.22	0.26	0.23	0.34	0.21	0.23	0.24	0.18	0.16
MgO	12.00	12.10	12.40	8.00	8.13	11.40	7.03	6.30	6.44	3.67	10.30	4.10
CaO	17.70	19.60	19.10	16.80	15.00	17.80	13.70	17.00	14.50	10.40	11.90	9.76
Na ₂ O	0.00	0.25	0.23	0.65	0.40	0.45	1.25	0.65	1.62	1.73	1.24	3.30
K ₂ O	0.28	0.06	0.00	0.76	1.56	0.41	1.48	0.96	0.98	4.83	0.99	1.36
P ₂ O ₅	0.02	0.00	0.00	0.09	1.12	0.10	0.81	0.06	0.40	0.51	0.07	0.26
H ₂ O	0.83	0.49	1.05	2.09	1.40	1.21	2.85	2.25	1.86	2.47	2.46	1.37
Sum	99.72	99.88	99.98	99.59	97.15	99.56	98.55	99.62	99.36	99.24	99.58	99.21
CIPW Norm												
or	1.33						9.14		5.94	29.49	6.02	8.21
ab							4.78		10.03	6.73	10.80	28.54
an	14.77	13.90	11.94	37.80	29.50	17.11	35.47	45.93	37.15	32.78	32.84	33.74
lc	0.27	0.28	0.05	3.61	7.55	1.93		4.57				
ne	0.01	1.15	1.07	3.06	1.91	2.10	3.40	3.06	2.18	4.55		
di	57.79	60.29	62.76	36.85	28.18	56.20	24.05	30.36	26.95	13.66	22.06	11.59
hy											13.23	11.44
ol	3.70	1.82	3.00	3.83	10.49	3.61	9.19	2.72	5.07	4.00	8.72	2.62
cs		2.02	1.19	0.08	1.67	0.14		0.55				
mt	20.32	18.80	18.41	12.76	15.38	16.70	10.15	11.23	10.10	6.38	4.78	2.19
il	1.76	1.72	1.59	1.79	2.60	1.97	1.87	1.44	1.64	1.20	1.39	1.05
ap	0.05			0.21	2.71	0.23	1.96	0.14	0.95	1.22	0.17	0.61
atomic ratio												
Mg												
(Mg+Fe ²⁺)	0.95	0.99	0.94	0.92	0.80	0.94	0.80	0.91	0.86	0.82	0.78	0.57
Ca												
(Ca+Na)	1.00	1.00	1.00	1.00	1.00	1.00	0.88	1.00	0.78	0.82	0.74	0.53

Rock types of analyzed samples in Tables 1-4. 86GH23A clinopyroxenite; 86GH25A clinopyroxenite; 86GH34B clinopyroxenite; 86GH20A clinopyroxenite; 86GH1B clinopyroxenite; 86GH35A gabbro; 86GH9B gabbro; 86GH8A clinopyroxenite; 86GH11A clinopyroxenite; 86GH12A melagabbro; 86GH7A melagabbro; 86GH1A gabbro; 86GH27A gabbro; 86GH3A melagabbro; 86GH30A gabbro; 86GH3B gabbro; 86GH8B diabase; 86GH14A diorite.

TABLE 2. CHEMICAL COMPOSITION OF CLINOPYROXENE IN THE SALT CHUCK INTRUSION

Sample	86GH 23A	86GH 25A	86GH 34B	86GH 20A	86GH 1B	86GH 35A	86GH 9B	86GH 8A	86GH 11A	Sample	86GH 12A	86GH 7A	86GH 1A	86GH 27A	86GH 3A	86GH 30A	86GH 3B	86GH 8B	86GH 14A
SiO ₂	48.60	48.90	48.82	49.45	48.88	49.96	49.84	49.53	48.51	SiO ₂	48.29	49.64	49.27	50.09	48.85	50.06	50.02	50.06	50.79
TiO ₂	0.53	0.50	0.64	0.42	0.81	0.44	0.59	0.62	0.59	TiO ₂	0.60	0.50	0.67	0.55	0.65	0.51	0.58	0.62	0.14
Al ₂ O ₃	4.78	4.47	4.65	4.16	4.47	3.89	4.10	4.35	5.07	Al ₂ O ₃	5.30	3.61	4.66	4.05	4.89	3.31	3.78	4.19	1.10
Cr ₂ O ₃	0.00	0.00	0.00	0.00	0.00	0.00	0.00	0.00	0.01	Cr ₂ O ₃	0.00	0.00	0.00	0.01	0.00	0.00	0.00	0.16	0.01
FeO	6.91	6.69	7.37	6.69	7.69	7.38	6.78	7.23	7.44	FeO*	8.04	7.27	7.10	7.17	7.49	7.31	8.10	8.41	11.16
MnO	0.16	0.18	0.35	0.14	0.34	0.41	0.37	0.34	0.24	MnO	0.24	0.42	0.33	0.36	0.26	0.35	0.60	0.21	0.58
MgO	14.15	14.31	14.16	14.34	13.75	13.92	14.56	14.11	13.39	MgO	12.92	14.15	13.91	14.30	13.44	14.47	13.40	15.51	13.51
CaO	23.72	23.57	23.00	23.53	23.22	22.71	22.74	23.25	23.34	CaO	23.55	22.96	23.05	22.96	23.16	22.22	22.04	20.15	20.70
Na ₂ O	0.23	0.22	0.35	0.27	0.42	0.71	0.34	0.36	0.38	Na ₂ O	0.46	0.38	0.38	0.40	0.43	0.47	0.58	0.24	0.24
Sum	99.08	98.63	99.32	99.00	99.36	99.11	99.12	99.79	98.98	Sum	99.40	98.92	99.38	99.89	99.17	98.69	99.10	99.53	98.20
Formula per 4 Cations										Formula per 4 Cations									
Si	1.808	1.822	1.813	1.839	1.818	1.859	1.844	1.832	1.811	Si	1.799	1.853	1.830	1.850	1.821	1.870	1.871	1.854	1.938
IVAl	0.192	0.178	0.187	0.161	0.192	0.141	0.158	0.168	0.189	IVAl	0.201	0.147	0.170	0.150	0.179	0.130	0.129	0.146	0.049
VIAl	0.017	0.019	0.017	0.022	0.014	0.021	0.024	0.021	0.035	VIAl	0.032	0.012	0.034	0.026	0.036	0.016	0.037	0.037	0.000
Ti	0.015	0.014	0.018	0.012	0.017	0.012	0.017	0.017	0.017	Ti	0.017	0.014	0.019	0.015	0.018	0.014	0.016	0.017	0.004
Cr	0.000	0.000	0.000	0.000	0.000	0.000	0.000	0.000	0.000	Cr	0.000	0.000	0.000	0.000	0.000	0.000	0.000	0.005	0.000
Fe ³⁺	0.162	0.147	0.160	0.135	0.165	0.147	0.124	0.138	0.147	Fe ³⁺	0.168	0.135	0.127	0.123	0.138	0.120	0.102	0.088	0.058
Fe ²⁺	0.053	0.062	0.069	0.073	0.074	0.082	0.087	0.085	0.085	Fe ²⁺	0.083	0.092	0.094	0.099	0.095	0.109	0.152	0.173	0.298
Mn	0.005	0.006	0.011	0.004	0.011	0.013	0.012	0.011	0.008	Mn	0.007	0.013	0.010	0.011	0.008	0.011	0.019	0.007	0.019
Mg	0.785	0.795	0.784	0.796	0.763	0.767	0.807	0.778	0.746	Mg	0.718	0.788	0.771	0.788	0.747	0.806	0.748	0.857	0.769
Ca	0.948	0.942	0.916	0.939	0.928	0.907	0.906	0.923	0.935	Ca	0.941	0.919	0.918	0.910	0.926	0.890	0.884	0.800	0.847
Na	0.017	0.016	0.025	0.019	0.030	0.051	0.025	0.028	0.027	Na	0.033	0.027	0.028	0.029	0.031	0.034	0.042	0.017	0.017
Sum	4.000	4.000	4.000	4.000	4.000	4.000	4.000	4.000	4.000	Sum	4.000	4.000	4.000	4.000	4.000	4.000	4.000	4.000	4.000
Mg (Mg+Fe ²⁺)										Mg (Mg+Fe ²⁺)									
	0.937	0.928	0.919	0.916	0.911	0.903	0.903	0.901	0.898		0.897	0.895	0.892	0.889	0.887	0.881	0.831	0.832	0.721
Es†	0.145	0.131	0.134	0.115	0.134	0.096	0.098	0.113	0.120	Es†	0.135	0.107	0.098	0.094	0.107	0.086	0.060	0.070	0.041
Wo	0.401	0.404	0.395	0.411	0.404	0.421	0.405	0.408	0.404	Wo	0.404	0.414	0.407	0.410	0.407	0.411	0.415	0.353	0.412
En	0.562	0.553	0.555	0.539	0.543	0.524	0.537	0.535	0.535	En	0.535	0.525	0.528	0.525	0.526	0.519	0.487	0.538	0.424
Fs	0.038	0.043	0.050	0.050	0.053	0.056	0.059	0.058	0.061	Fs	0.062	0.062	0.065	0.066	0.067	0.070	0.099	0.109	0.164

* Total iron calculated as FeO; Fe³⁺ and Fe²⁺ in mineral formulae calculated from charge balance.

† Es, Wo, En and Fs calculated according to the procedures of Lindsley & Andersen (1983). See Table 1 for rock types.

the high oxygen fugacity of the magma, as indicated by crystallization of abundant magnetite, structural formulae for clinopyroxene were calculated by normalizing to four cations, and Fe³⁺ and Fe²⁺ were calculated from charge balance. Although calculation of Fe³⁺ and Fe²⁺ by this procedure is subject to bias resulting from errors in the analysis, particularly for Si, it is superior in this case to assuming all iron as FeO or Fe₂O₃. For hornblende, the best formula was obtained by normalizing to 13 cations exclusive of Ca, Na, and K, and assigning cations to sites according to the method outlined by Robinson *et al.* (1982). Biotite formulae were calculated by normalizing to 11 atoms of oxygen with all iron as FeO, which obviously introduces some error.

With the classification scheme of the International Mineralogical Association (Morimoto *et al.* 1988), all the clinopyroxene compositions in the Salt Chuck intrusion would be classified as diopside. However, the clinopyroxene in magnetite clinopyroxenite and gabbro has a substantial Fe³⁺ content; in all but one case, Fe³⁺ is greater than Fe²⁺. Most of the Fe³⁺ in the clinopyroxene is in the esseneite component, which is not taken into account in the IMA classification scheme. Thus we calculated the Wo, En, and Fs components of clinopyroxene (Table 2) using the projection scheme of Lindsley & Andersen (1983). This procedure shows that

quadrilateral components make up only 76.5 to 80.3% of total quadrilateral and other components, and that the esseneite component ranges from 14.5 to 6.0%. When projected onto the pyroxene quadrilateral, the clinopyroxene samples plot as Mg-rich augite (Fig. 3).

The Mg# of the modal clinopyroxene in magnetite clinopyroxenite and gabbro ranges from 0.94 to 0.83, indicating a substantial chemical trend due to differentiation. The Mg# of pyroxene in the diorite is 0.72. Although not regular, there is also a general decrease in proportion of the esseneite component of clinopyroxene with differentiation. Inspection of Tables 1 and 2 shows that there is generally a good correlation between the Mg# of the modal clinopyroxene and the normative clinopyroxene. Exceptions are samples 86GH8A and 86GH7A, which have a lower Mg# in normative clinopyroxene owing to the presence of significant bornite and chalcopyrite. The generally good correlation between Mg# of modal and normative clinopyroxene indicates that the Fe²⁺/Fe³⁺ ratio in clinopyroxene calculated by charge balance is consistent with the FeO/Fe₂O₃ ratio determined by analysis of the rocks. The general agreement of Mg# also suggests that the FeO and Fe₂O₃ values determined for the rocks are close to primary values and have not been significantly affected by alteration.

TABLE 3. CHEMICAL COMPOSITION OF HORNBLende IN GABBRO AND DIORITE OF THE SALT CHUCK INTRUSION

Sample	86GH9B	86GH14A
SiO ₂	40.04	41.79
TiO ₂	2.15	1.98
Al ₂ O ₃	13.19	9.48
FeO*	13.00	20.43
MnO	0.25	0.32
MgO	12.97	9.31
CaO	12.31	10.90
Na ₂ O	2.56	1.74
K ₂ O	1.31	0.99
Sum	97.79	96.94
Si	5.939	6.338
IVAl	2.061	1.662
Sum T	8.000	8.000
VIAl	0.245	0.034
Ti	0.241	0.226
Fe ³⁺	0.429	0.924
Fe ²⁺	1.185	1.668
Mn	0.031	0.041
Mg	2.869	2.106
Sum C	5.000	5.000
Ca	1.959	1.774
Na	0.041	0.226
Sum B	2.000	2.000
Na	0.697	0.286
K	0.249	0.192
Sum A	0.946	0.478
$\frac{\text{Mg}}{\text{(Mg+Fe}^{2+}\text{)}}$	0.708	0.558

* Total iron calculated as FeO. Fe³⁺ and Fe²⁺ in mineral formula calculated from charge balance. Mineral formula normalized to 13 cations exclusive of Ca, Na, and K.

The pyroxene compositions given in Table 2 and plotted in Figure 3 are averages of several grains per sample. There is no significant variation among average grain compositions in a given sample, but individual

TABLE 4. CHEMICAL COMPOSITION OF BIOTITE IN THE SALT CHUCK INTRUSION

Sample	86GH8A	86GH9B	86GH12A	86GH14A
SiO ₂	36.64	35.76	36.26	35.09
TiO ₂	4.03	3.70	3.58	3.73
Al ₂ O ₃	16.55	16.93	17.10	14.68
FeO*	10.99	12.06	13.04	23.89
MnO	0.17	0.19	0.20	0.18
MgO	17.59	17.47	16.00	9.43
CaO	0.04	0.15	0.10	0.04
Na ₂ O	0.62	0.39	0.27	0.13
K ₂ O	8.56	7.90	7.72	8.31
Sum	95.18	94.53	94.26	95.47
Cations per 11 Oxygens				
Si	2.683	2.642	2.689	2.730
IVAl	1.317	1.358	1.311	1.270
VIAl	0.111	0.117	0.183	0.076
Ti	0.222	0.205	0.200	0.218
Fe	0.673	0.745	0.809	1.554
Mn	0.011	0.012	0.013	0.012
Mg	1.919	1.924	1.768	1.094
Ca	0.003	0.012	0.008	0.003
Na	0.088	0.056	0.039	0.020
K	0.799	0.744	0.730	0.824
Sum	7.825	7.815	7.749	7.801
$\frac{\text{Mg}}{\text{(Mg+Fe)}}$	0.740	0.721	0.686	0.413

* Total iron calculated as FeO. See Table 1 for rock types.

grains commonly show concentric zoning, with Mg# decreasing slightly toward the rim. The maximum difference in Mg# between the interior and rim of a single grain is about 0.05, and generally it is less than 0.02.

Hornblende is rare and generally occurs only in trace amounts. Using the classification of Leake (1978) as modified by Hawthorne (1981), the one amphibole analyzed in a gabbro is magnesio-hastingsite; hornblende in the diorite is tschermakitic (Table 3). Mg# for the biotite in magnetite clinopyroxenite and gabbro ranges from about 0.74 to 0.69; in diorite, the Mg# is about 0.41 (Table 4). The TiO₂ content of biotite ranges from 3.73 to 4.03 wt. %.

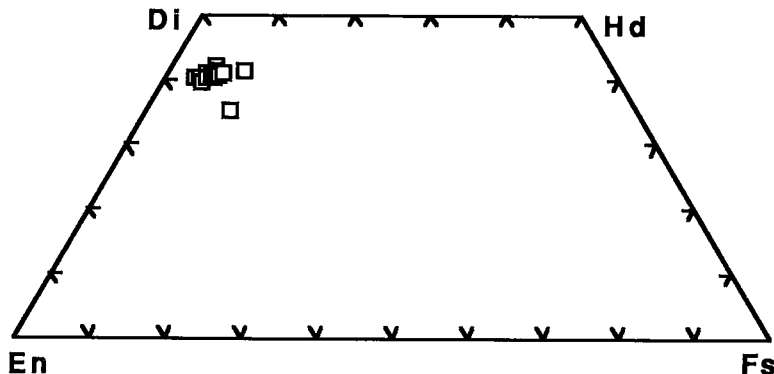


FIG. 3. Compositions of clinopyroxene in the Salt Chuck intrusion projected onto the pyroxene quadrilateral. Wo, En, and Fs components were calculated using the projection scheme of Lindsley & Andersen (1983).

PETROGENESIS

Conditions of crystallization

The temperature, pressure, water content, and oxygen fugacity during crystallization of the Salt Chuck intrusion can be qualitatively estimated by comparing the natural mineral assemblages and crystallization sequence to products of hydrous melting and crystallization experiments using natural basaltic compositions. The order of crystallization indicated by magnetite clinopyroxenite and gabbro in the Salt Chuck intrusion is clinopyroxene + magnetite followed by plagioclase. Hornblende occurs only in trace amounts, and biotite nearly always is postcumulus. The abundance of magnetite and the common occurrence of biotite indicate that the magma that crystallized to form the ultramafic rocks was substantially rich in Fe^{3+} and H_2O . Experimental studies have shown that under water-saturated and -undersaturated conditions and an oxygen fugacity at the NNO buffer, plagioclase and hornblende crystallize after clinopyroxene and magnetite (Holloway & Burnham 1972, Helz 1973, Allen & Boettcher 1978). At moderate to high pressures, hornblende crystallizes at a temperature substantially higher than the temperature at which plagioclase crystallizes, but at low pressures (2–3 kbar), the upper stability of plagioclase and hornblende are relatively close, and below about 2.5 kbar, plagioclase crystallizes before hornblende (Holloway & Burnham 1972). Furthermore, at pressures below 2 kbar, the upper stability of hornblende is very near the temperature of the solidus (Holloway & Burnham 1972), a condition that would restrict crystallization of hornblende. Thus, the sequence of crystallization and the near-absence of hornblende in the Salt Chuck intrusion suggest that it crystallized under low pressure, probably 2 kbar or less. Alternatively, the near-absence of hornblende could indicate a water content below that required for saturation of hornblende, but in view of the common occurrence of biotite, this interpretation seems unlikely.

The occurrence of cumulus magnetite with cumulus clinopyroxene suggests that the state of oxidation of the magma at the time of crystallization was at least as high as the NNO buffer. For basaltic melts under oxidizing conditions equivalent to the NNO buffer, magnetite crystallizes after clinopyroxene but prior to plagioclase (Holloway & Burnham 1972, Helz 1973). At less oxidizing conditions, the FMQ buffer, ilmenite is the near-liquidus phase. At conditions of the HM buffer, Fe–Ti oxide phases are among the earliest to crystallize but they include abundant titaniferous hematite (Helz 1973), which was not observed in the Salt Chuck intrusion. The fact that Fe^{3+} exceeds Fe^{2+} in clinopyroxene also suggests a relatively high fugacity of oxygen during crystallization. However, the general decrease in the essenite component of clinopyroxene with differentiation suggests that the redox state of the magma decreased as fractional crystallization proceeded. Re-

duction of the magma during fractional crystallization would be expected in response to magnetite crystallization. Similar oxidizing conditions near the NNO buffer were reported for ultramafic xenoliths in arc basalt that have mineral assemblages similar to Alaskan-type ultramafic rocks (Arculus & Wills 1980, Conrad & Kay 1984).

The occurrence of cumulus magnetite and the absence of cumulus plagioclase in the magnetite clinopyroxenite suggest a temperature of crystallization below 1090°C but above 1025°C; these values correspond to the upper stability limits of magnetite and plagioclase, respectively, in hydrous basalt magma at 2 kbar and at the NNO buffer (Holloway & Burnham 1972). In those rare gabbros where hornblende is a minor cumulus phase, the temperature of crystallization must have decreased to at least 975°C, which is the upper stability of hornblende at 2 kbar and NNO (Holloway & Burnham 1972). The upper stability of magnetite and plagioclase decreases, and that of hornblende increases, with increasing pressure but, as discussed above, the sequence of crystallization suggests that the pressure of crystallization was probably near 2 kbar.

Nature of parent magma

The Alaskan-type bodies have long been recognized as a distinct class of ultramafic–mafic intrusions (Noble & Taylor 1960, Taylor & Noble 1960, Irvine 1974), and the nature of the parental magma has long been debated. No chilled margins representing the parental magma have been found; thus the composition of the original melt could only be inferred from consideration of cumulate sequences and from rock and mineral chemistry relative to experimental and theoretical studies. James (1971), Murray (1972), Himmelberg *et al.* (1986) and, more recently, Loucks (1990) argued that at least some of the Alaskan-type ultramafic rocks fractionated from subalkaline, orthopyroxene-normative, island-arc basaltic parental magmas, with the resultant production of residual basaltic and andesitic liquids. Subalkaline, island-arc basaltic parental magmas for Alaskan-type ultramafic rocks also were implied by Conrad & Kay (1984) and DeBari *et al.* (1987) in equating xenoliths in Aleutian arc volcanic rocks with Alaskan-type ultramafic rocks. Irvine (1967, 1974), on the other hand, argued that the Alaskan-type ultramafic rocks were fractionated from high-Ca, high-Mg, alkaline ultrabasic parental magmas, with the resulting production of residual, critically undersaturated alkali basalts. Irvine's (1974) argument for a silica-undersaturated alkaline ultrabasic parental magma was based in part on normative nepheline in rocks with abundant postcumulus hornblende. Loucks (1990), however, pointed out that the experimental studies of Bowen (1928), Helz, (1973) and Wones (1979) all showed that hornblende precipitated from orthopyroxene- or quartz-normative melts is generally nepheline-normative. Thus hornblende- or

biotite-bearing cumulates that crystallized from saturated hydrous magmas will commonly be feldspathoid-normative.

In the case of the Salt Chuck intrusion, the mineral assemblages, the sequence of crystallization, and the rock and mineral chemistry all indicate fractionation from a silica-saturated, orthopyroxene-normative parental magma similar to those that yield island-arc basalts. As discussed above, the Salt Chuck mineral assemblages and sequence of crystallization are duplicated by crystallization experiments on hydrous, silica-saturated basaltic melts at low pressures (≈ 2 kbar) and oxygen fugacity near that of the NNO buffer (Holloway & Burnham 1972). The experimental studies of Helz (1973) on the hydrous system, although at higher pressure (5 kbar), also support our interpretation.

The Salt Chuck magnetite clinopyroxenites and gabbros are feldspathoid-normative (Table 1). However, as mentioned above, this is a result of the substantial esseneite component ($\text{CaFe}^{3+}\text{AlSiO}_6$) of the clinopyroxene, which is a result of the hydrous, oxidizing nature of the magma (Loucks 1990). Loucks argued that in a hydrous and oxidizing basaltic magma, the activity of the enstatite component would be depressed, and the activities of the aluminous pyroxene components in both melt and clinopyroxene crystals would be raised. Thus

early-crystallized clinopyroxene from such magmas is characteristically aluminous, and particularly enriched in the esseneite component. The esseneite component calculates in the norm as magnetite plus silica-undersaturated components. Clinopyroxene compositions reported by Holloway & Burnham (1972) and Helz (1973) from their experimental crystallization of hydrous silica-saturated basalts are generally not feldspathoid-normative; however, the clinopyroxene encountered in experiments generally coexists with hornblende, which incorporates those components that calculate as normative feldspathoids. The virtual absence of hornblende in the Salt Chuck crystallization sequence resulted in the normative feldspathoid components entering clinopyroxene.

Crystallization of the Salt Chuck mineral assemblages from anhydrous island-arc basaltic magma also is supported by the studies of Loucks (1990), which showed that clinopyroxene in arc cumulates has a distinctive trend in terms of Al/Ti ratio. Figure 4 shows that the Salt Chuck clinopyroxenes fall on the arc cumulate trend.

If the isolated exposure of diorite is an evolved product of fractionation of the Salt Chuck parent magma, then that parent magma was unquestionably silica-saturated. The rock and mineral chemistry of the diorite,

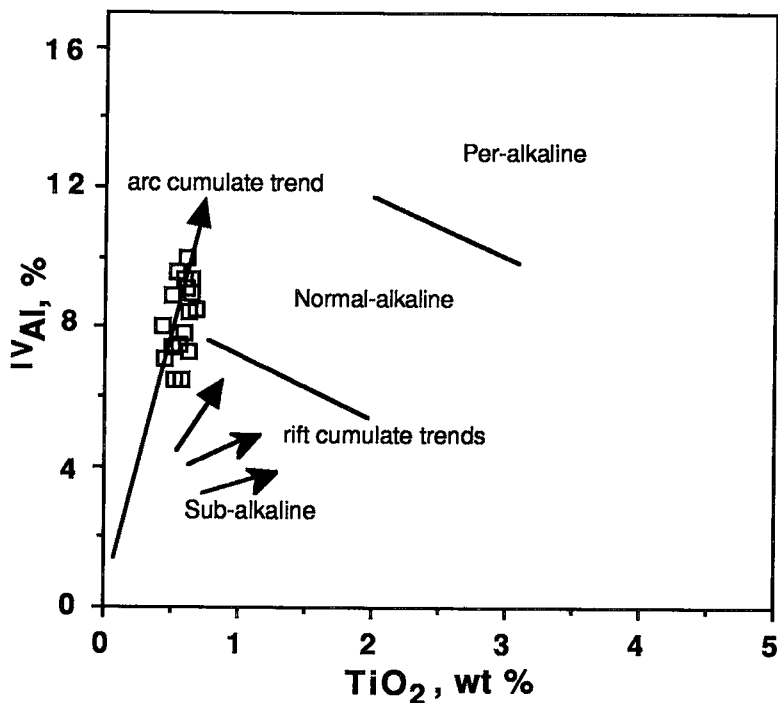


FIG. 4. Plot of ^{IV}Al content, expressed as a percentage of total Al, against TiO_2 for clinopyroxene in the Salt Chuck intrusion. Field boundaries are from LeBas (1962), and trends are from Loucks (1990).

including a significant proportion of the esseneite component in the pyroxene, is supportive of this interpretation, but unfortunately no contacts between the diorite and gabbro or magnetite clinopyroxenite are exposed, and thus a genetic relationship cannot be unequivocally demonstrated.

As mentioned above, no chilled margins or other representatives of parental magma for the Alaskan-type ultramafic bodies have ever been found. However, it is plausible that the diabase dike (sample 86GH8B) that intrudes Salt Chuck magnetite clinopyroxenite may represent the nearly direct crystallization of the Salt Chuck parental magma. The diabase dike has a normative $Mg\#$ of 0.78, which is appropriate to be in exchange equilibrium with clinopyroxene with a $Mg\#$ of 0.90 to 0.94 typical of the magnetite clinopyroxenite (Table 2). The $Fe^{2+}/\Sigma Fe$ atomic ratio of the diabase dike is 0.707, which corresponds to a silicate liquid with an oxygen fugacity of NNO plus 1 or 2 log units (Sack *et al.* 1980, Carmichael & Ghiorso 1986); this value is about the same as the oxygen fugacity indicated for the magma that crystallized the magnetite clinopyroxenites and gabbros. The diabase dike is hypersthene-normative and not too dissimilar in chemical composition from the 1921 Kiluea olivine tholeiite used in the hydrous experiments of Holloway & Burnham (1972) and Helz (1973). Thus the diabase dike has an appropriate chemical composition, $Mg\#$, and redox state to represent a plausible parental liquid to the mineral assemblages at Salt Chuck.

We believe that the Salt Chuck data indicate that the magnetite clinopyroxenite and gabbro fractionated from a hydrous basaltic liquid and that this parental liquid is closely represented by the composition of the diabase dike that intrudes the magnetite clinopyroxenite. These conclusions have implications for the origin of high-alumina and calc-alkaline basalts. Loucks (1990) argued that for hydrous basaltic liquids under oxidizing conditions, early fractionation of clinopyroxene enriched in the esseneite component has the consequence of enhancing the alumina and silica content of progressive residual liquids, thus leading to crystallization of high-alumina basalts and calc-alkaline basalt. Our study of the Salt Chuck intrusion, especially our documentation of crystallization of esseneite-rich clinopyroxene from a parental magma that most likely had a hydrous, highly oxidizing basaltic composition, supports the arguments of Loucks (1990) for the importance of fractionation of subsilicic clinopyroxene in the derivation of calc-alkaline and high-alumina basalts.

ORE DEPOSITS

The commercial (Au+Pd)-bearing copper sulfide deposit associated with the Salt Chuck intrusion differs markedly from the known PGE occurrences in other Alaskan-type ultramafic bodies in southeast Alaska. Typically, the Alaskan-type ultramafic bodies have

noncommercial concentrations of Pt-dominant PGE that are associated with olivine-rich rocks in which sulfides are generally scarce. Iron, in the form of magnetite, is the only commodity that has attracted commercial interest (Ruckmick & Noble 1959). These characteristics also apply to Alaskan-type ultramafic intrusions elsewhere, such as in the Klamath Mountains (Gray *et al.* 1986) and in British Columbia (Findlay 1969). Where commercial PGE deposits do occur in Alaskan-type intrusions, as in the Urals (Razin 1976, Naldrett & Cabri 1976), they are associated with olivine-rich rocks containing concentrations of either chromite or magnetite. It seems, therefore, that the abundance of sulfide and the absence of olivine in the Salt Chuck intrusion are anomalies among the Alaskan-type intrusions in general.

The Salt Chuck ore deposit is located in the eastern middle part of the intrusion, as indicated by the location of the Salt Chuck mine (Fig. 2). This mine, the only one that has worked the deposit, operated intermittently from 1905 to 1941 and produced about 300,000 metric tonnes of milling ore (chiefly bornite and chalcocopyrite in magnetite clinopyroxenite) estimated to have averaged 0.95 wt% Cu, 14.91 g Au, 7.04 g Ag, and 26.1 g Pd per tonne (Holt *et al.* 1948, Gault 1945). Recent exploration has been undertaken by Silver Glimpse Resources Inc. (formerly Orbex Industries Inc.).

Grades are higher and sulfide mineral aggregates are larger in the magnetite clinopyroxenite, in which unevenly distributed, irregular, interstitial grains of bornite occur in modal amounts as much as 15 vol.%. In the generally lower-grade gabbro ore, the bornite grains are smaller and more evenly distributed. Chalcocopyrite, although widely distributed, is a minor component of the ore, being largely confined to fault zones. Alteration products are chalcocite, covellite, and digenite. Small flakes of native Cu are widespread, but of little economic importance. Other elements associated with the Cu sulfides are recoverable amounts of Au, Ag, Pd, and minor Pt. In addition, Pt-group minerals (PGM) probably form an important source of PGE in the ore. Watkinson & Melling (1989) described a complex texture, consisting of abundant, large, mostly isolated grains of PGM, consisting mostly of kotulskite (PdTe), which are either intergrown with hessite (Ag_2Te), or rimmed or entirely replaced by temagamite (Pd_3HgTe_3). Also occurring as free aggregates or within sulfide grains are complex intergrowths of Au-bearing sperrylite ($PtAs_2$) + kotulskite + Pd_6AsSb , temagamite + Au, and kotulskite + temagamite + merenskyite ($PdTe_2$).

Based on megascopic observations, Gault (1945) suggested that the ore-bearing fluids followed the contact and spread into the fractured magnetite clinopyroxenite and the less-fractured gabbro. The influence of the gabbro – magnetite clinopyroxenite contact on ore deposition has been recently affirmed by Watkinson & Melling (1989). According to Gault (1945), the more prominent faults (some containing chalcocopyrite) may

have been the main channel for dispersion of copper-bearing fluids to smaller faults and fractures, and thence to microfractures observed in the rock at Salt Chuck by Mertie (1969). Mertie suggested that, although the sulfides appear megascopically to be magmatic segregations, numerous microscopic cracks were adequate for circulation of ore solutions. According to Mertie, the degree of alteration appears to be a function of ore grade, supporting a hydrothermal origin.

It is our view that the predominantly disseminated character of the sulfides and PGM, together with the igneous textures of the host rocks, indicate that the segregations were produced by late magmatic hydrothermal processes in a single intrusive event, probably the same event that produced the extensive deuteric alteration of the silicates. Veins and fracture-fillings were produced at this later stage within the magmatic environment. The presence of abundant Pd-rich minerals (Watkinson & Melling 1989) suggests late stages of PGE mineralization, in which palladium went into PGM rather than into sulfides (Stumpfl & Tarkian 1976). Late-stage, lower-temperature PGE mineralization (<720°C) in the Salt Chuck deposit also is indicated by the presence of the Pd bismuthotelluride minerals such

as merenskyite, kotulskite, and temagamite (Sweeny *et al.* 1989).

Recently Watkinson & Melling (1989) described aggregates of sulfide minerals at Salt Chuck with relict magmatic textures that range from disseminated to net textures. These are composed of complex intergrowths and concentric assemblages of chalcopyrite – bornite – digenite – chalcocite with euhedral epidote.

In our view, the Salt Chuck deposit was probably formed by a two-stage process: (1) a magmatic stage of crystallization in which the sulfides and PGE accumulated in a disseminated manner in cumulus deposits, possibly largely in the gabbro, and (2) a later magmatic–hydrothermal stage during which the sulfides and PGE were remobilized and concentrated in veins and fracture-fillings, largely in the magnetite clinopyroxenite but controlled by the complex magnetite clinopyroxenite – gabbro contact. In this model, the source of the sulfides and PGE was the magma that produced the Salt Chuck intrusion, in agreement with the suggestion of Gault (1945).

Table 5 gives a summary of the analytical data on the PGE for both the Salt Chuck intrusion and the Cretaceous Alaskan-type ultramafic intrusions of southeast-

TABLE 5. PLATINUM-GROUP ELEMENT ANALYSES OF ULTRAMAFIC AND MAFIC ROCKS IN THE SALT CHUCK INTRUSION AND CRETACEOUS ALASKAN-TYPE INTRUSIONS IN SOUTHEASTERN ALASKA†

LOCALITY	ROCK TYPE**	Pt	Pd	Rh	Ru	Ir	Cu	Ni	Au	$\frac{\text{Cu}}{\text{(Cu+Ni)}}$	$\frac{\text{Pt}}{\text{(Pt+Pd)}}$	$\frac{\text{Pd}}{\text{(Pd+Rh)}}$	$\frac{\text{Rh}}{\text{(Rh+Ru)}}$
CRETACEOUS ALASKAN-TYPE													
DUKE ISLAND † Max.(22)	Prd/Cpx	200	140	10							0.59		
DUKE ISLAND † Av. (22)	Prd/Cpx	37	33	0							0.53		
UNION BAY † Max. (50)	Prd/Cpx	1600	200	62		215					0.89		
UNION BAY † Av. (50)	Prd/Cpx	93	23	0							0.80		
BLASHKE IS † Max. (10)	Prd/Cpx	20	20	0							0.50		
BLASHKE IS † Av. (10)	Prd/Cpx	10	10	0							0.50		
KLUKWAN † Max. (10)	Cpx	100	100	0							0.50		
KLUKWAN † Av. (10)	Cpx	46	40	0							0.53		
KLUKWAN † #	Cpx	9.5	14	0							0.40		
HAINES † #	Cpx	48	27	0.9							0.64		
HAINES † #	Hbd	44	51	1.2							0.46		
UNION BAY 87GH27A	Du	12	0.8	0.8	1.5	2.1					0.94	0.50	0.35
UNION BAY 87GH34A	Whr	8.5	0	1.7	0.8	6.1					1.00	0.00	0.68
UNION BAY 87GH44A	Gb	2.3	9.5	0	0	0					0.19	1.00	
UNION BAY 87GH47A	Cpx	7.3	3.9	0.6	0	0					0.65	0.87	1.00
UNION BAY 87GH40A	Hbd	0.9	1.1	0	0	0					0.45	1.00	
UNION BAY 87GH41A	Cpx	7.9	11	0	0.5	0					0.42	1.00	0.00
AVERAGE ALASKAN-TYPE RATIOS											0.59	0.73	0.51
SALT CHUCK													
87GH42A	Cpx	19	840	0	0	0					0.02		
87GH43A	Cpx	4.4	51	0	0	0					0.08		
SALT CHUCK † Max. (6)	Cpx	160	2900	0							0.05		
SALT CHUCK † Av. (6)	Cpx	57	1010	0							0.05		
SCM † Av.(32)	Cpx	37.7	1230				7001	24	314	1.00	0.03		
SCM Av.(35)	Gb	7.17	201				1575	18	181	0.99	0.03		
AVERAGE SALT CHUCK RATIOS											0.99	0.05	

† All analyses in parts per billion, except Cu, Ni, and Au in wt %. Av. = average; Max. = maximum; (22) = number of specimens.

** Prd, peridotite; Cpx, clinopyroxenite; Hbd, hornblende; Du, dunite; Whr, wehrlite; Gb, gabbro.

* Analyses from Clark and Greenwood (1972).

Analyses from A.B. Ford (written communication, 1991).

†SCM. Analyses from Salt Chuck Mine, courtesy Silver Glance Resources Inc. (formerly Orbx Industries Inc.).

87GH**** Specimens collected by the authors.

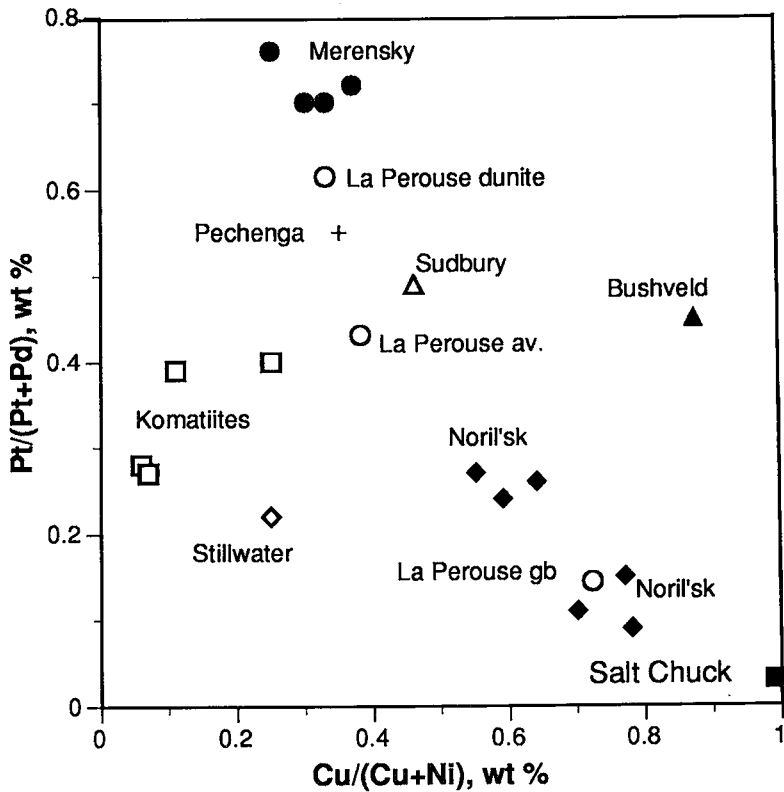


FIG. 5. Plot of Pt/(Pt+Pd) for magnetite clinopyroxenite and gabbro of the Salt Chuck intrusion (see Table 5 for data) compared with world-wide data adapted from Naldrett & Cabri (1976). Data for the La Perouse gabbro from Czamanske *et al.* (1981).

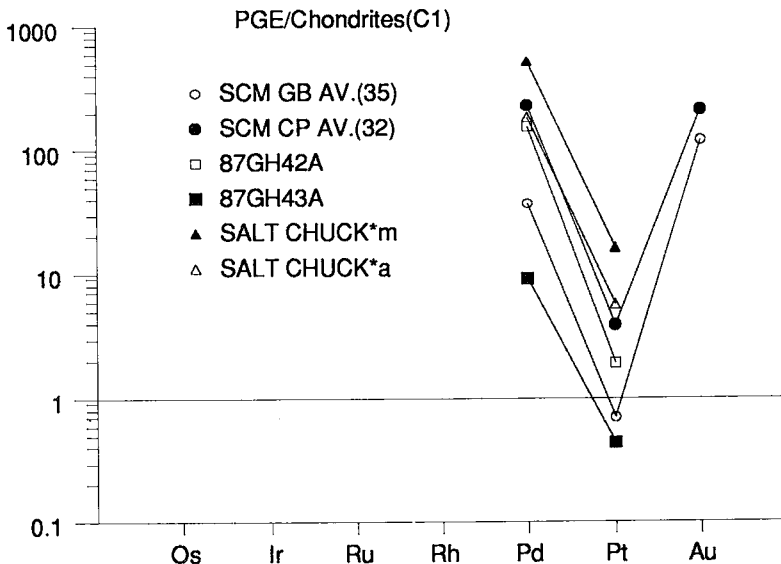


FIG. 6. Chondrite-normalized Pd, Pt, and Au data (Table 5) for the Salt Chuck intrusion. Chondrite (C-1) values from Naldrett & Duke (1980); plotting program from Wheatley & Rock (1988).

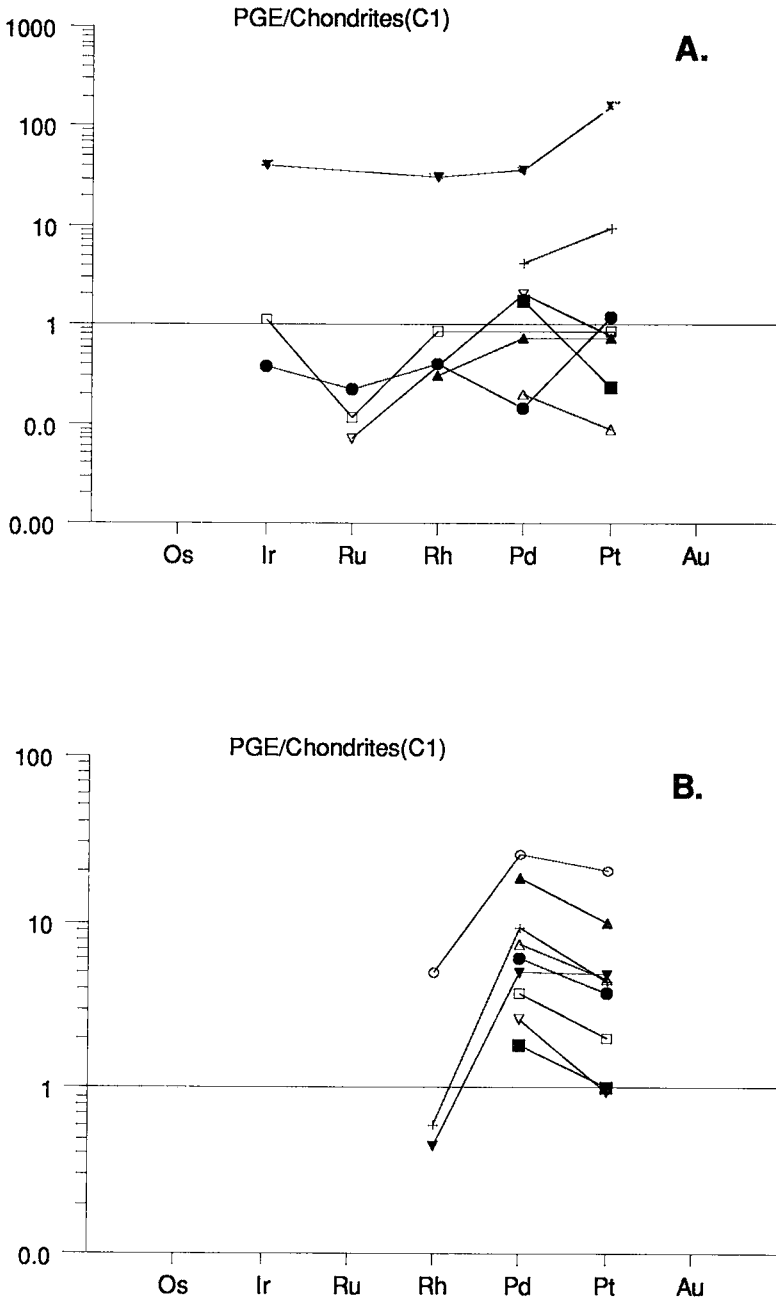


FIG. 7. Chondrite-normalized PGE diagrams for Alaskan-type ultramafic intrusions, southeastern Alaska. Construction of diagrams as in Figure 6. A. Union Bay: ● 87GH27A, □ 87GH34A, ■ 87GH44A, ▲ 87GH47A, △ 87GH40A, ▼ 87GH41A, ∇ Union Bay* Max., + Union Bay* Av. B. ○ Duke Island* Max., ● Duke Island* Av., □ Blashke Is.* Av., ▲ Klukwan* Max., △ Klukwan* Av., ∇ Klukwan#, ▼ Haines# cpx, + Haines# hbl. See Table 5 for data and key.

ern Alaska. From these data, it is clear that the dominance of Pd over Pt [average $Pt/(Pt+Pd) = 0.06$] in the Salt Chuck intrusion contrasts sharply with the general dominance of Pt over Pd [average $Pt/(Pt+Pd) = 0.59$] in other Alaskan-type bodies. Also evident are the generally higher levels of PGE concentrations in the Salt Chuck deposit, which also contains a much higher concentration of sulfide. The Salt Chuck data are also compared (Fig. 5) to the $Cu/(Cu + Ni)$ and $Pt/(Pt + Pd)$ ratios of sulfide ores associated with other ultramafic rocks (Naldrett & Cabri 1976). Sulfides in the Salt Chuck intrusion are substantially more Cu- and Pd-rich than magmatic sulfides in other ultramafic rocks, and plot at the high-Pd and high-Cu corner of Figure 5. The atypically high $Cu/(Cu+Ni)$ ratio in the magnetite clinopyroxenite might be attributed to the two-stage model proposed above. The high fugacity of oxygen of the magma would have suppressed early precipitation of sulfides (Katsura & Nagashima 1974, Carroll & Rutherford 1988) and allowed Ni to enter early-crystallizing silicates and oxides. Consequently, the sulfides or sulfide liquid that precipitated from the evolved gabbroic magma would have been Cu-enriched. Subsequent remobilization of the sulfides or sulfide liquid into the magnetite clinopyroxenite by magmatic-hydrothermal processes would then yield sulfides with a $Cu/(Cu+Ni)$ ratio that would be atypical for the host rock.

Naldrett (1981) concluded that PGE concentrate in sulfide droplets by a factor of 100 to 1000 over their levels in the host magma. Recent experimental work by Stone *et al.* (1990) has shown that PGE+Au are strongly partitioned into sulfide liquid. According to them, the sulfide liquid – silicate melt partition coefficients (D values) for the noble metals are $9 (\pm 7) \times 10^4$ for Pd, $9 (\pm 0.7) \times 10^5$ for Ir, $9 (\pm 6) \times 10^3$ for Pt, and $1 (\pm 0.9) \times 10^3$ for Au. According to these data, the affinity of Pd and Ir for sulfide liquid is about 50 times greater than that of Pt and about 500 times greater than that of Au. This relation is supported by the data from the Salt Chuck mine, where rocks richer in sulfides are richer in Pd and also Au (Table 5, see Cu content *versus* Pd; Holt *et al.* 1948, Gault 1945). This sulfide-collector process could explain the higher PGE+Au content in the sulfide-rich Salt Chuck intrusion than in the other, sulfide-poor Alaskan-type intrusions in southeastern Alaska. Figures 6 and 7 graphically compare the PGE patterns of Salt Chuck samples with other Alaskan-type bodies of southeastern Alaska by means of normalized diagrams based on the computer program of Wheatley & Rock (1988) and the chondrite data from Naldrett & Duke (1980). These figures show the general dominance of Pd over Pt and the generally higher concentration of PGE in the Salt Chuck intrusion. However, data for the less-abundant PGE are limited, and the analytical data are not of uniform quality. For this reason, it is not possible to make a detailed comparison of the normalized PGE patterns within the region, much less with the rest of the world. For example, the PGE data from the

Union Bay body are especially conflicting, and suggest a need for further study.

CONCLUSIONS

The early Paleozoic Salt Chuck intrusion has petrographic and chemical characteristics that are similar to those of Cretaceous Alaskan-type ultramafic-mafic bodies. The intrusion consists almost entirely of magnetite clinopyroxenite and gabbro cumulates. Field relationships and sequences of cumulus minerals indicate that the two rock types are related by fractional crystallization. Relationships in the mine suggest the existence of cyclic units produced by multiple emplacement of magma batches. A petrogenetically significant feature of the intrusion is that all the samples analyzed are feldspathoid-normative; four samples of magnetite clinopyroxenite and two of gabbro are even larnite-normative. The presence of silica-undersaturated components in the norm is a result of the high proportion of the esseneite component ($CaFe^{3+}AlSiO_6$) in clinopyroxene in these rocks, and not a indication of crystallization from a silica-undersaturated magma. The Mg# values of the normative and modal clinopyroxene show a good correlation and a substantial range, consistent with a normal trend of fractional crystallization. Although not regular, there is also a general decrease in the proportion of the esseneite component of clinopyroxene with differentiation, suggesting reduction of the magma as crystallization proceeded. Comparison of the natural assemblages of minerals and sequence of crystallization to products of experiments on hydrous melting and crystallization using natural basaltic compositions suggests that the Salt Chuck intrusion crystallized under low pressures, probably 2 kbar or less, with oxidation conditions near those of the NNO buffer. Temperatures of crystallization probably decreased from about 1090°C for the magnetite clinopyroxenites to approximately 975°C for some hornblende-bearing gabbros.

Mineral assemblages, sequence of crystallization, and rock and mineral chemistry all indicate fractionation from a hydrous, silica-saturated, orthopyroxene-normative parental magma similar to those that yield island-arc basalts. The orthopyroxene-normative diabase dike that intrudes magnetite clinopyroxenite has an appropriate chemical composition, Mg#, and redox state to represent a plausible parental liquid to the Salt Chuck mineral assemblages. The commercial Au+Pd-bearing copper sulfide deposit associated with the Salt Chuck intrusion differs markedly from the known occurrences of PGE in other Alaskan-type ultramafic bodies in southeast Alaska. Pt-group minerals (PGM) probably form an important source of PGE in the ore. The Salt Chuck deposit is Pd-dominant, has higher concentrations of PGE and sulfides, and the sulfides are substantially more Cu- and Pd-rich than magmatic sulfides in other ultramafic rocks. We conclude that the Salt Chuck deposit was probably formed by a two-stage process: (1) a stage

of magmatic crystallization in which the sulfides and PGE accumulated in a disseminated manner in cumulus deposits, possibly largely in the gabbro, and (2) a later magmatic-hydrothermal stage during which the sulfides and PGE were remobilized and concentrated in veins and fracture-fillings, largely in the magnetite clinopyroxenite but controlled by the complex magnetite clinopyroxenite – gabbro contact. In this model, the source of the sulfides and PGE was the magma that produced the Salt Chuck intrusion.

Although the Salt Chuck intrusion generally has been considered as an Alaskan-type intrusion and shows many similarities to other Alaskan-type bodies, we do not propose that the conditions of crystallization, composition of parent magma, and ore-forming processes inferred for the Salt Chuck intrusion are universally applicable to all intrusions classified as being of Alaskan type.

ACKNOWLEDGEMENTS

We thank Dr. Peter E. Fox of Silver Glance Resources (formerly Orbex Industries Inc.), of Vancouver, B.C., for his courtesy in granting us access to the Salt Chuck property, and for providing us with chemical data. Thanks also are due to the following colleagues at the U.S. Geological Survey: G.K. Czamanske and T.E. Keith for their helpful reviews of the paper, and Floyd Gray for providing us with information on the mine. We especially thank R.F. Martin, G.T. Nixon, and an anonymous reviewer whose thorough and constructive reviews provided new insights and led to a much improved paper.

REFERENCES

- ALBEE, A.L. & RAY, L. (1970): Correction factors for electron probe microanalysis of silicates, oxides, carbonates, phosphates, and sulfates. *Anal. Chem.* **42**, 1408-1414.
- ALLEN, J.C. & BOETTCHER, A.L. (1978): Amphibole in andesite and basalt. II. Stability as a function of P - T - f_{H_2O} - f_{O_2} . *Am. Mineral.* **63**, 1074-1087.
- ARCULUS, R.J. & WILLS, K.J.A. (1980): The petrology of plutonic blocks and inclusions from the Lesser Antilles island arc. *J. Petrol.* **21**, 743-799.
- BENCE, A.E. & ALBEE, A.L. (1968): Empirical correction factors for the electron microanalysis of silicates and oxides. *J. Geol.* **76**, 382-403.
- BERG, H.C., JONES, D.L. & CONEY, P.J. (1978): Pre-Cenozoic tectonostratigraphic terranes of southeastern Alaska and adjacent areas. *U.S. Geol. Surv. Open-File Rep.* **78-1085** (2 sheets).
- BOWEN, N.L. (1928): *The Evolution of the Igneous Rocks*. Princeton Univ. Press, Princeton, New Jersey.
- BREW, D.A. & FORD, A.B. (1984): Tectonostratigraphic terranes in the Coast plutonic-metamorphic complex, southeastern Alaska and northwestern British Columbia. *U.S. Geol. Surv., Circ.* **939**, 90-93.
- _____ & MORRELL, R.P. (1984): Intrusive rocks and plutonic belts of southeastern Alaska, U.S.A. *Geol. Soc. Am., Mem.* **159**, 171-193.
- BUDDINGTON, A.F. & CHAPIN, R. (1929): Geology and mineral deposits of southeastern Alaska. *U.S. Geol. Surv., Bull.* **800**.
- CARMICHAEL, I.S.E. & GHIORSO, M.S. (1986): Oxidation-reduction relations in basic magma: a case for homogeneous equilibria. *Earth Planet. Sci. Lett.* **78**, 200-210.
- CARROLL, M.R. & RUTHERFORD, M.J. (1988): Sulfur speciation in hydrous experimental glasses of varying oxidation state: results from measured wavelength shifts of sulfur X-rays. *Am. Mineral.* **73**, 845-849.
- CLARK, A.L. & GREENWOOD, W.R. (1972): Geochemistry and distribution of platinum-group metals in mafic to ultramafic complexes of southern and southeastern Alaska. *U.S. Geol. Surv., Prof. Pap.* **800-C**, 157-160.
- CONRAD, W.K. & KAY, R.W. (1984): Ultramafic and mafic inclusions from Adak Island: crystallization history, and implications for the nature of primary magmas and crustal evolution in the Aleutian arc. *J. Petrol.* **25**, 88-125.
- CZAMANSKE, G.K., HAFFTY, J. & NABBS, S.W. (1981): Pt, Pd, and Rh analyses and beneficiation of mineralized mafic rocks from the La Perouse layered gabbro, Alaska. *Econ. Geol.* **76**, 2001-2011.
- DEBARI, S., KAY, S.M. & KAY, R.W. (1987): Ultramafic xenoliths from Adagdak volcano, Adak, Aleutian Islands, Alaska: deformed igneous cumulates from the moho of an island arc. *J. Geol.* **95**, 329-341.
- EBERLEIN, G.D. & CHURKIN, M., JR. (1970): Paleozoic stratigraphy in the northwest coastal area of Prince of Wales Island, southeastern Alaska. *U.S. Geol. Surv., Bull.* **1284**.
- _____, _____, CARTER, C., BERG, H.C. & OVENSINE, A.T. (1983): Geology of the Craig quadrangle, Alaska. *U.S. Geol. Surv., Open-File Rep.* **83-91**.
- FINDLAY, D.C. (1969): Origin of the Tulameen ultramafic-gabbro complex, southern British Columbia. *Can. J. Earth Sci.* **6**, 399-425.
- GAULT, H.R. (1945): The Salt Chuck copper-palladium mine, Prince of Wales Island, southeastern Alaska. *U.S. Geol. Surv., Open-File Rep.* **46-19**.
- _____ & WAHRHAFTIG, C. (1992): The Salt Chuck copper-palladium mine, Prince of Wales Island, southeastern Alaska. War Minerals Report for Federal War Agencies (1943). *U.S. Geol. Surv., Open-File Rep.* **92-293**.
- GEHRELS, G.E. & SALEEBY, J.B. (1987a): Geologic framework,

- tectonic evolution, and displacement history of the Alexander terrane. *Tectonics* **6**, 151-173.
- _____ & _____ (1987b): Geology of southern Prince of Wales Island, southeastern Alaska. *Geol. Soc. Am., Bull.* **98**, 123-137.
- GRAY, F., PAGE, N.J., CARLSON, C.A., WILSON, S.A. & CARLSON, R.R. (1986): Platinum-group element geochemistry of zoned ultramafic intrusive suites, Klamath Mountains, California and Oregon. *Econ. Geol.* **81**, 1252-1260.
- HAWTHORNE, F.C. (1981): Crystal chemistry of the amphiboles. In *Amphiboles and Other Hydrous Pyriboles - Mineralogy* (P.H. Ribbe, ed.). *Rev. Mineral.* **9A**, 1-102.
- HELZ, R.T. (1973): Phase relations of basalts in their melting range at $P_{H_2O} = 5$ kb as a function of oxygen fugacity. I. Mafic phases. *J. Petrol.* **14**, 249-302.
- HIMMELBERG, G.R., LONEY, R.A. & CRAIG, J.T. (1986): Petrogenesis of the ultramafic complex at the Blashke Islands, southeastern Alaska. *U.S. Geol. Surv., Bull.* **1662**.
- HOLLOWAY, J.R. & BURNHAM, C.W. (1972): Melting relations of basalt with equilibrium water pressure less than total pressure. *J. Petrol.* **13**, 1-29.
- HOLT, S.P., SHEPARD, J.G., THORNE, R.L., TOLONEN, A.W. & FOSSE, E.L. (1948): Investigation of the Salt Chuck copper mine, Kasaan Peninsula, Prince of Wales Island, southeastern Alaska. *U.S. Bur. Mines, Rep. Invest.* **4358**.
- IRVINE, T.N. (1967): The Duke Island ultramafic complex, southeastern Alaska. In *Ultramafic and Related Rocks* (P.J. Wyllie, ed.). John Wiley & Sons, New York (84-97).
- _____ (1974): Petrology of the Duke Island ultramafic complex, southeastern Alaska. *Geol. Soc. Am., Mem.* **138**.
- JAMES, O.B. (1971): Origin and emplacement of ultramafic rocks of the Emigrant Gap area, California. *J. Petrol.* **12**, 523-560.
- KATSURA, T. & NAGASHIMA, S. (1974): Solubility of sulfur in some magmas at 1 atm pressure. *Geochim. Cosmochim. Acta* **38**, 517-531.
- KENNEDY, G.C. & WALTON, M.S., JR. (1946): Geology and associated mineral deposits of some ultrabasic rock bodies in southeastern Alaska. *U.S. Geol. Surv., Bull.* **947-D**, 65-84.
- LAMPHERE, M.A. (1968): Sr-Rb-K and Sr isotopic relationships in ultramafic rocks, southeastern Alaska. *Earth Planet. Sci. Lett.* **4**, 185-190.
- _____ & EBERLEIN, G.D. (1966): Potassium-argon ages of magnetite-bearing ultramafic complexes in southeastern Alaska. *Geol. Soc. Am., Spec. Pap.* **87**, 94 (abstr.).
- LEAKE, B.E. (1978): Nomenclature of amphiboles. *Am. Mineral.* **63**, 1023-1052.
- LE BAS, M.H. (1962): The role of aluminum in igneous clinopyroxenes with relation their parentage. *Am. J. Sci.* **260**, 267-288.
- LEECH, G.B., LOUDON, J.A., STOCKWELL, C.H. & WANLESS, R.K. (1963): Age determinations and geological studies. *Geol. Surv. Can., Pap.* **63-17**.
- LINDSLEY, D.H. & ANDERSEN, D.J. (1983): A two pyroxene thermometer. *Proc. 13th Lunar Planet. Sci. Conf.* **2**; *J. Geophys. Res.* **88**, Supplement, A887-A906.
- LONEY, R.A., HIMMELBERG, G.R. & SHEW, N. (1987): Salt Chuck palladium-bearing ultramafic body, Prince of Wales Island. *U.S. Geol. Surv., Circ.* **995**, 126-127.
- LOUCKS, R.R. (1990): Discrimination of ophiolitic from non-ophiolitic ultramafic-mafic allochthons in orogenic belts by the Al/Ti ratio in clinopyroxene. *Geology* **18**, 346-349.
- MERTIE, J.B., JR. (1969): Economic geology of the platinum metals. *U.S. Geol. Surv., Prof. Pap.* **630**.
- MORIMOTO, N., FABRIES, J., FERGUSON, A.K., GINZBURG, I.V., ROSS, M. SEIFERT, F.A., ZUSSMAN, J., AOKI, K. & GOTTARDI, G. (1988): Nomenclature of pyroxenes. *Am. Mineral.* **73**, 1123-1133.
- MURRAY, C.G. (1972): Zoned ultramafic complexes of the Alaskan type: feeder pipes of andesitic volcanoes. *Geol. Soc. Am., Mem.* **132**, 313-335.
- NALDRETT, A.J. (1981): Platinum-group element deposits. In *Platinum-Group Elements: Mineralogy, Geology, Recovery* (L.J. Cabri, ed.). *Can. Inst. Min. Metall., Spec. Vol.* **23**, 197-231.
- _____ & CABRI, L.J. (1976): Ultramafic and related mafic rocks: their classification and genesis with special reference to the concentration of nickel sulfides and platinum-group elements. *Econ. Geol.* **71**, 1131-1158.
- _____ & DUKE, J.M. (1980): Platinum metals in magmatic sulfide ores. *Science* **208**, 1417-1424.
- NOBLE, J.A. & TAYLOR, H.P., JR. (1960): Correlation of the ultramafic complexes of south eastern Alaska with those of other parts of north America and the world. *Int. Geol. Congr., 21st* **13**, 188-197.
- PALMER, A.R. (1983): The decade of North American geology 1983 geologic time scale. *Geology* **11**, 503-504.
- RAZIN, L.V. (1976): Geologic and genetic features of forsterite dunites and their platinum-group mineralization. *Econ. Geol.* **71**, 1371-1376.
- ROBINSON, P., SPEAR, F.S., SCHUMACHER, J.C., LAIRD, J., KLEIN, C., EVANS, B.W. & DOOLAN, B.L. (1982): Phase relations of metamorphic amphiboles: natural occurrence and theory. In *Amphiboles: Petrology and Experimental Phase Relations* (D.R. Veblen & P.H. Ribbe, eds.). *Rev. Mineral.* **9B**, 1-227.

- RODDICK, J.C. & FARRAR, E. (1971): High initial argon ratios in hornblendes. *Earth Planet. Sci. Lett.* **12**, 208-214.
- _____ & _____ (1972): Potassium-argon ages of the Eagle granodiorite, southern British Columbia. *Can. J. Earth Sci.* **9**, 596-599.
- RUBLEE, J. & PARRISH, R.R. (1990): Chemistry, chronology and tectonic significance of the Tulameen complex, southwestern British Columbia. *Geol. Assoc. Can. - Mineral. Assoc. Can., Program Abstr.* **14**, A114.
- RUCKMICK, J.C. & NOBLE, J.A. (1959): Origin of the ultramafic complex at Union Bay, southeastern Alaska. *Geol. Soc. Am., Bull.* **70**, 981-1018.
- SACK, R.O., CARMICHAEL, I.S.E., RIVERS, M. & GHIORSO, M.S. (1980): The ferrous-ferric equilibria in natural silicate liquids at 1 kbar. *Contrib. Mineral. Petrol.* **75**, 369-376.
- SAINSBURY, C.L. (1961): Geology of part of the Craig C-2 quadrangle and adjoining areas, Prince of Wales Island, southeastern Alaska. *U.S. Geol. Surv., Bull.* **1058-H**, 299-362.
- SALEEBY, J.B. & EBERLEIN, G.D. (1981): An ensimatic basement complex and its relation to the early Paleozoic volcanic-arc sequence of southern Prince of Wales Island, southeastern Alaska. *Geol. Soc. Am., Abstr. Programs* **13**, 104.
- STONE, W.E., CROCKET, J.H. & FLEET, M.E. (1990): Partitioning of palladium, iridium, platinum, and gold between sulfide liquid and basalt at 1200°C. *Geochim. Cosmochim. Acta* **54**, 2341-2344.
- STUMPFL, E.F. & TARKIAN, M. (1976): Platinum genesis: new mineralogical evidence. *Econ. Geol.* **71**, 1451-1460.
- STURROCK, D.L., ARMSTRONG, R.L. & MAXWELL, R.B. (1980): Age and Sr isotopic composition of the Pyroxenite Creek ultramafic complex, southwestern Yukon: an Alaskan-type ultramafic intrusion. *Geol. Surv. Can., Pap.* **80-1B**, 185-188.
- SWEENEY, J.M., EDGAR, A.D., CHARBONNEAU, H.E. & MCHARDY, D.C. (1989): Platinum group minerals (PGM) as indicators of magmatic vs hydrothermal processes: evidence from the Lac des Iles and Rathbun Lake, Ontario platinum group element deposits (PGE). *Geol. Assoc. Can. - Mineral. Assoc. Can., Program Abstr.* **14**, A48-A49.
- TAYLOR, H.P., JR. (1967): The zoned ultramafic complexes of southeastern Alaska. In *Ultramafic and Related Rocks* (P.J. Wyllie, ed.). John Wiley & Sons, New York (97-121).
- _____ & NOBLE, J.A. (1960): Origin of the ultramafic complexes in southeastern Alaska. *Int. Geol. Congr., 21st* **13**, 175-187.
- WALTON, M.S. (1951): The Blashke Islands ultrabasic complex, with notes on related areas in southeastern Alaska. *U.S. Geol. Surv., Open-File Rep.* **126**, 266.
- WATKINSON, D.H. & MELLING, D.R. (1989): Genesis of Pd-Pt-Au-Ag-Hg minerals in Cu-rich sulfides; Salt Chuck mafic ultramafic rock complex, Alaska. *Geol. Assoc. Can. - Mineral. Assoc. Can., Program Abstr.* **14**, A48.
- WHEATLEY, M. & ROCK, N.M.S. (1988): SPIDER: A MacIntosh program to generate normalized multi-element "spidergrams". *Am. Mineral.* **73**, 919-921.
- WONES, D.R. (1979): The fractional resorption of complex minerals and the formation of strongly femic alkaline rocks. In *The Evolution of the Igneous Rocks: Fiftieth Anniversary Perspectives* (H.S. Yoder, Jr., ed.). Princeton University Press, Princeton, New Jersey (413-422).

Received May 22, 1991, revised manuscript accepted December 16, 1991.